Hindawi
Geofluids
Volume 2021, Article ID 6664164, 15 pages
https://doi.org/10.1155/2021/6664164

Research Article

Hydrogeochemistry and Groundwater Quality Assessment in the High Agri Valley (Southern Italy)

M. Paternoster,[1,2] **R. Buccione**,[1] **F. Canora**,[3] **D. Buttitta**,[1] **S. Panebianco**,[1,4] **G. Rizzo**,[1] **R. Sinisi**,[4] **V. Summa**,[4] **and G. Mongelli**[1,4]

[1]*Department of Sciences, University of Basilicata, Vialedell'AteneoLucano 10, Campus Macchia Romana, 85100 Potenza, Italy*
[2]*National Institute of Geophysics and Volcanology (INGV), Section of Palermo, 90153 Palermo, Italy*
[3]*School of Engineering, University of Basilicata, Viale dell'Ateneo Lucano 10, Campus Macchia Romana, 85100 Potenza, Italy*
[4]*National Research Council, Institute of Methodologies for Environmental Analysis (CNR-IMAA), 85050 Tito Scalo (PZ), Italy*

Correspondence should be addressed to M. Paternoster; michele.paternoster@unibas.it

Received 22 October 2020; Revised 18 December 2020; Accepted 7 June 2021; Published 25 June 2021

Academic Editor: Orlando Vaselli

The High Agri Valley (southern Italy) is one of the largest intermontane basin of the southern Apennines affected by intensive agricultural and industrial activities. The study of groundwater chemical features provides much important information useful in water resource management. In this study, hydrogeochemical investigations coupled with multivariate statistics, saturation indices, and stable isotope composition (δD and δ^{18}O) were conducted in the High Agri Valley to determine the chemical composition of groundwater and to define the geogenic and anthropogenic influences on groundwater quality. Twenty-four sampling point (including well and spring waters) have been examined. The isotopic data revealed that groundwater has a meteoric origin. Well waters, located on recent alluvial-lacustrine deposits in shallow porous aquifers at the valley floor, are influenced by seasonal rainfall events and show shallow circuits; conversely, spring waters from fissured and/or karstified aquifers are probably associated to deeper and longer hydrogeological circuits. The *R*-mode factor analysis shows that three factors explain 94% of the total variance, and F1 represents the combined effect of dolomite and silicate dissolution to explain most water chemistry. In addition, very low contents of trace elements were detected, and their distribution was principally related to natural input. Only two well waters, used for irrigation use, show critical issue for NO_3^- concentrations, whose values are linked to agricultural activities. Groundwater quality strongly affects the management of water resources, as well as their suitability for domestic, agricultural, and industrial uses. Overall, our results were considered fulfilling the requirements for the inorganic component of the Water Framework Directive and Italian legislation for drinking purposes. The water quality for irrigation is from "good to permissible" to "excellent to good" although salinity and relatively high content of Mg^{2+} can occasionally be critical.

1. Introduction

Groundwater resource is one of the most challenging current and future issues of worldwide concern. The ever-increasing rate of population growth and the inherent water supply demand have led to intensive water exploitation. Groundwater is of great importance for domestic, drinking, irrigation, and industry purposes especially where the water resource is availability scarce. Groundwater quality depends on natural processes such as rock-water interaction, climatic conditions, geological context, and anthropogenic activities. Natural processes including the mineral precipitation or dissolution, ion-exchange, redox condition, residence time, and mixing between different water type may have a great impact on groundwater quality [1]. Anthropogenic activities such as rapid urbanization, industrialization, and intensive agricultural activities have caused a deterioration in water quality worldwide [2–5]. Groundwater contamination can be persisted a long time due to the low flow rate of groundwater in an aquifer and may involve major ions and trace elements [6]. High levels of contaminants, exceeding guideline values, can turn water to be unsuitable for drinking, irrigation, fishing,

and recreation [7], causing serious adverse effects on human and biota health [8]. The release of elements from rocks depends upon physical (temperature, residence time, flow rate) and chemical factors (namely, weathering of rock-forming minerals, precipitation of sparingly soluble secondary minerals, and presence of reactive gas species such as CO_2), i.e., [9, 10]. The redox process can have an important role in determining the partitioning between aqueous solution and solid phases, taking into account that some elements are present in nature in different oxidation states. In southern Apennines (southern Italy), the High Agri Valley (hereafter HAV) is characterized by a relevant presence of intensive agricultural activities in predominantly hilly environment due to the occurrence of groundwater and fertile soils and a unique forest heritage with a rich biodiversity that have stimulated tourism growth. In recent decades, together with an ancient rural economy based on agriculture, wood, and dairy production, new industrial activities have been undertaken. Hydrocarbon extraction, related to the largest onshore oil field in Western Europe, is the most important industrial activity and has actually an oil production capacity of about 80.000 barrels/day [11]. In the HAV, the groundwater represents an important freshwater resource, used as drinking water supply for agricultural and industrial purposes. Usually, the anthropogenic activities influencing groundwater systems contribute to a decrease in water availability, both directly through variations in aquifer recharge and indirectly through changes in groundwater quality and use. The evaluation and management of groundwater resources require an understanding of hydrogeochemical features of the aquifers.

The aim of this research, representing the first step of a comprehensive hydrogeochemical characterization of the area, is to understand the geochemical evolution of groundwater in the HAV in order to guarantee reliable supply for all purposes and define a sustainable groundwater management strategy, also considering the growing industrialization that could cause pollution phenomena. The main objectives are to (1) determine the geochemical processes controlling the chemical composition, (2) define the geogenic and anthropogenic influences on groundwater quality, and (3) compare the concentrations of some inorganic elements to values established by the World Health Organization and the Italian legislation for drinking and irrigation purposes.

2. Climate, Geology, and Hydrogeology

HAV area (Basilicata region, southern Italy) extends for about 140 km^2 and is 30 km long and 12 km wide. According to the Köppen classification, the climate of the area is of warm-summer Mediterranean type, characterized by cold-humid winter and hot-dry summer. In the study area, the mean annual precipitation value (calculated in 2005-2015 range) was of about 1000 mm/y, while the mean annual temperature was of 12.5°C. The coldest month was January with average temperature ranging between 3°C and 4°C. Hot and arid conditions during summer produce periods of drought during July and August. The climate of the area, characterized by high seasonal precipitation rates in autumn and spring and snowy winter, allows the greatest amount of the aquifer recharge. From a geological point of view, HAV is a NW-SE trending Quaternary basin located in the axial zone of the southern Apennines, an east-verging fold-and-thrust belt developed as an accretionary wedge due to the eastward migration of the compressional tectonics in the Apennine Arc (Late Oligocene-Early Pleistocene) [12, 13]. The HAV evolution, since the Middle Pleistocene, is controlled by a still active NE-SW extensional tectonic regime [14], as witnessed by NW striking high-angle normal and oblique faults bordering the basin, which represent the main seismogenic structures in the area [15, 16]. The HAV is characterized by Quaternary continental deposits overlying a Pre-Quaternary substratum (Figure 1(a)). In the south-west side of the basin, the substratum consists of Mesozoic to Cenozoic shallow-water and slope carbonates of the Campania–Lucania Platform over thrusted on coeval pelagic successions (Lagonegro Units), while to south-east the substratum is characterized by Tertiary siliciclastic sediments of the Gorgoglione Flysch and Albidona Formation [13, 17]. A Quaternary synorogenic succession, consisting of Lower Pleistocene-Holocene continental clastic sediments, mainly coarse-grained, fills the HAV basin [18] and references therein. Finally, the most recent Pleistocene and Holocene deposits are represented by terraced alluvium, alluvial fans, and recent to present-day alluvial sediments (Figure 1(a)).

The HAV hydrogeology is characterized by a high groundwater content favoured by climate conditions. Two different kinds of aquifers are recognized: fissured and/or karstified aquifers in the Apennine units of the substratum and porous multilayer aquifers developed in the Quaternary succession [19]. Both types host high volumes of groundwater storage, with the richest amount located in Pre-Quaternary substratum aquifers usually subdivided in different hydrogeological complexes according to the structural, lithological, and permeability features [20]. These aquifers mainly occur in highly fractured limestones (Carbonate Platform) and in the underlying "Calcari con Selce" Fm (Lagonegro Units), both characterized by high permeability (Figure 1(b)). Porous aquifers occur in gravelly-sandy permeable deposits of the Quaternary succession [21], where the larger groundwater body is recognized in a multilayered and semiconfined aquifer. Carbonate karst and fractured aquifers play a leading role in the overall hydrogeological system, since their groundwater resources supply the detrital-alluvial ones occurring at the valley bottom. Finally, most springs from HAV, generally showing an average flow rate greater than 5 l/s, are at the contact between permeable limestone and dolostone (Lagonegro Units and Carbonate Platform) and impermeable Plio-Pleistocene siliciclastic and recent alluvial-lacustrine deposits [22].

3. Materials and Methods

3.1. Sampling and Analyses. Twenty-four water samples were collected during a single survey carried out between March and April 2016 in the HAV. Nine of them were taken from springs of the fissured and/or karstified aquifers located on Pre-Quaternary carbonate rocks and sediments belonging to the Lagonegro Units and fifteen from wells on recent alluvial-lacustrine deposits in shallow porous aquifers at the valley floor with a phreatic level ranging from 1 to 6 meters

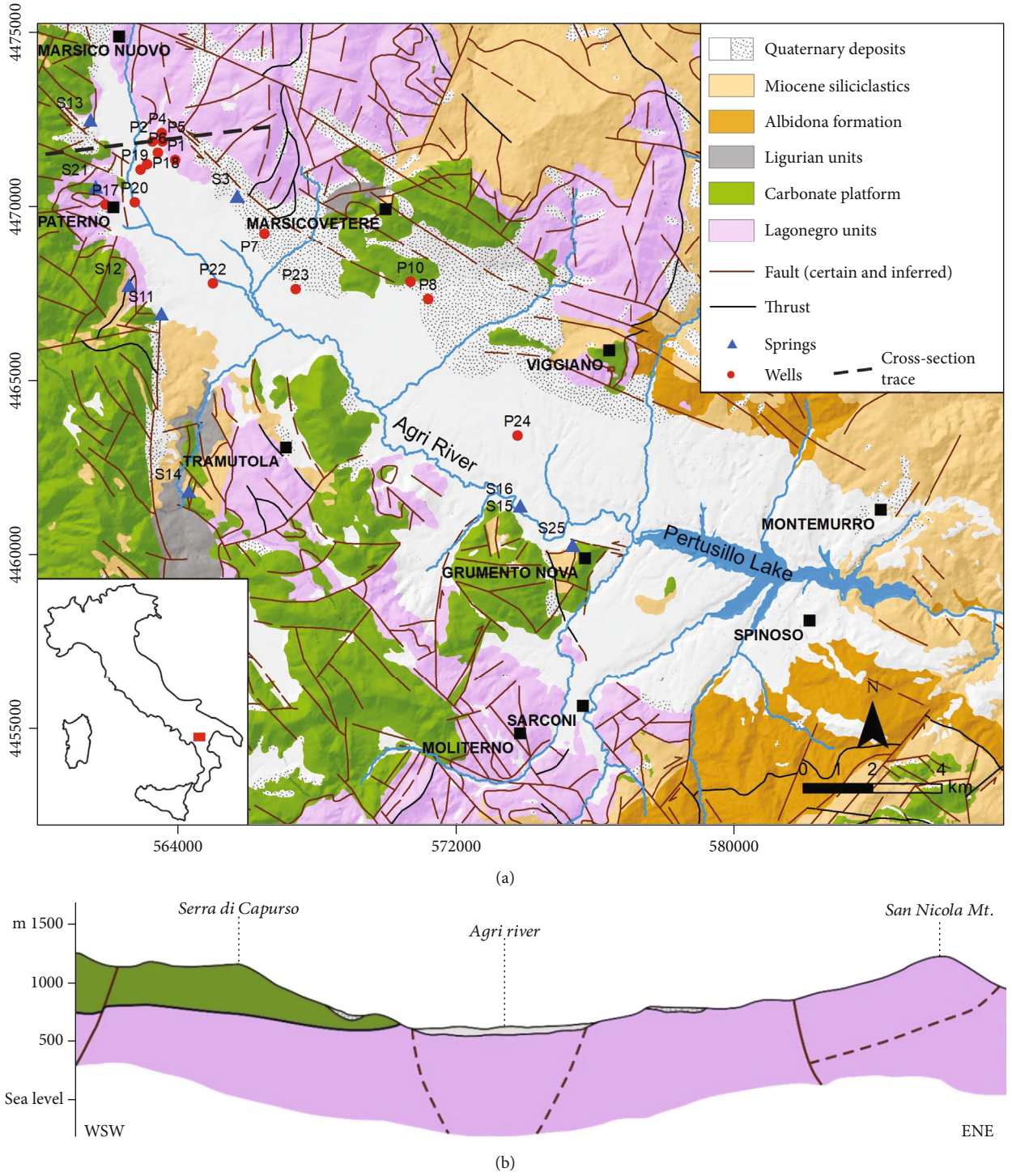

FIGURE 1: Geological sketch map (a) of the investigated area (modified after Giocoli et al. [15]) where localization of the sampling sites (springs and wells) is displayed. Schematic cross section (b) of the northern part of study area is drawn (modified after Carbone et al. [17]).

from the surface (Figure 1). The investigated springs are located on the right bank of the Agri River, except for S3 site, in the left river side. Most of springs, managed by the Acquedotto Lucano public agency, are used for drinking purposes, whereas well waters, mostly belonging to private individuals, are used for irrigation purposes. Temperature, pH, electric conductivity (EC, measured at 25°C), and redox potential (Eh) were measured in situ using a high-resolution multiparametric probes (Hanna Instruments HI-9828), after calibration in the laboratory by means PTB/NIST traceable standard solutions. Total alkalinity was determined in situ by titrating unfiltered samples with 0.01 N HCl, and methyl-orange was indicator. All water samples were filtered in situ at 0.45 μm membrane (MF-Millipore) and then stored in low-density

Table 1: Location (latitude and longitude by WGS84-33T), water type (W: well; S: spring), physico-chemical parameters (T, pH, Eh, TDS), major elements (from Ca^{2+} to HCO_3^-), and irrigation quality parameters (SAR, MAR, %Na, RSBC, PI) of the investigated groundwaters. Spring water is from fissured and/or karstified aquifer, while well waters from shallow porous aquifer.

ID	Lat.	Long.	Type	*T* °C	pH	EC µS/cm	Eh mV	TDS mg/l	Na^+ mg/l	K^+ mg/l	Ca^{2+} mg/l	Mg^{2+} mg/l	SiO_2 mg/l	Cl- mg/l	NO_3^- mg/l	NO_2^- mg/l	SO_4^{2-} mg/l	HCO_3^- mg/l	IB %	SAR meq/l	MAR %	Na %	RSBC meq/l	PI %
P1	563935	4471312	W	21	6.51	837	720	647	8.5		5.4	107	9.7	10.8	3.7	b.d.l.	14.7	488	4.1	0.2	97.0	3.9	7.7	34.0
P2	563284	4471850	W	16.5	6.8	681	760	585	9.0		12.2	91	10.6	9.1	b.d.l.	b.d.l.	26.4	427	4.1	0.2	92.5	4.6	6.4	35.9
P4	563554	4472085	W	15	7.05	522	783	434	7.9		9.7	63	8.0	7.0	b.d.l.	b.d.l.	34.0	305	0.8	0.2	91.4	5.7	4.5	43.0
P5	563572	4471846	W	19.5	6.75	869	800	812	32.8		17.8	108	14.3	32.4	58	b.d.l.	47.3	502	0.5	0.6	90.9	12.8	7.3	38.4
P6	563444	4471523	W	20	6.82	710	750	631	13.7	1.6	13.3	96	12.0	13.4	3.4	b.d.l.	40.4	439	4.0	0.3	92.2	6.9	6.5	35.9
P7	566491	4469202	W	18.5	7.05	1000	752	748	25.3	16.5	20.8	100	17.1	26.9	203	b.d.l.	61.7	293	1.3	0.5	88.8	14.1	3.8	31.7
P8	571209	4467296	W	16.5	6.95	620	770	541	7.1	1.4	11.6	82	17.3	7.9	21.0	b.d.l.	16.7	378	3.6	0.2	92.1	4.5	5.6	36.8
P10	570710	4467800	W	16.4	6.79	578	722	481	14.8	1.7	12.1	68	14.5	12.6	13.4	b.d.l.	16.0	329	4.6	0.4	90.3	9.9	4.8	43.2
P17	561946	4470037	W	19	6.9	617	755	538	10.4		18.3	77	16.4	11.9	7.5	b.d.l.	6.8	390	4.6	0.2	87.3	5.9	5.5	38.9
P18	563128	4471200	W	16.6	6.32	770	370	657	16.1	1.7	16.4	90	22.3	15.3	b.d.l.	b.d.l.	45.7	451	1.1	0.3	90.1	8.3	6.6	38.3
P19	562941	4471047	W	22.7	6.79	579	483	499	7.4	1.13	19.0	68	9.1	8.0	b.d.l.	b.d.l.	9.5	378	2.0	0.2	85.6	5.1	5.3	40.8
P20	562786	4470103	W	18.2	6.45	453	530	385	8.1	6.1	18.2	49	9.6	10.3	19.6	b.d.l.	13.8	256	3.4	0.2	81.7	9.3	3.3	45.3
P22	565018	4467747	W	18.4	7.05	566	240	504	21.0		25.2	57	13.7	6.9	b.d.l.	b.d.l.	2.8	378	3.0	0.5	78.8	13.3	4.9	49.7
P23	567389	4467585	W	19.4	6.86	765	668	679	10.6	1.1	25.7	96	10.7	8.5	3.6	b.d.l.	24.1	500	3.6	0.2	86.0	5.1	6.9	34.5
P24	573780	4463398	W	16.5	6.91	577	570	511	20.8		11.5	67	15.3	8.6	3.7	b.d.l.	6.8	378	2.4	0.5	90.6	13.0	5.6	48.7
S3	565710	4470285	S	18	7.39	365	730	330	5.3	1.1	7.8	51	6.9	6.6	2.2	b.d.l.	6.8	244	5.1	0.2	91.5	5.3	3.6	46.4
S11	563543	4466886	S	11.5	7.3	317	680	303	3.2		11.9	44	4.7	4.5	b.d.l.	b.d.l.	3.4	232	4.0	0.1	85.8	3.2	3.2	48.2
S12	562611	4467695	S	12	7.1	340	760	305	3.2		9.6	46	4.7	4.2	2.5	b.d.l.	3.5	232	4.5	0.1	88.8	3.2	3.3	47.4
S13	561505	4472467	S	11.3	7.13	346	750	307	3.7		11.0	45	5.9	5.0	b.d.l.	b.d.l.	4.2	232	4.8	0.1	87.1	3.6	3.2	47.6
S14	564327	4461796	S	11	7.11	388	675	340	3.4		14.6	49	5.2	5.1	3.4	b.d.l.	3.4	256	4.6	0.1	84.7	3.0	3.5	44.8
S15	573856	4461380	S	14.1	6.87	560	774	473	7.3	1.8	18.6	64	8.8	8.1	5.2	b.d.l.	6.9	354	2.1	0.2	85.0	5.5	4.9	41.8
S16	573856	4461380	S	16.2	7.06	500	790	424	6.3		16.1	60	8.5	6.9	4.2	b.d.l.	5.9	317	3.4	0.2	85.9	4.6	4.4	42.7
S21	561657	4470549	S	14	6.76	442	738	435	14.4	1.36	18.5	55	10.5	6.9	2.4	b.d.l.	9.6	317	3.9	0.4	83.1	10.8	4.3	47.8
S25	575348	4460258	S	13.5	6.7	585	732	484	9.9	3.17	15.9	64	11.1	9.8	10.2	b.d.l.	9.0	354	0.8	0.2	87.0	7.8	5.0	43.5
d.l.									0.9	1.0	0.5	0.6	3.0	1.6	1.9	0.9	1.5	n.d.						

EC: electrical conductivity measured at 25°C; *T*: temperature; Eh: redox potential; TDS: total dissolved solid; d.l.: detection limit; b.d.l.: below detection limit; IB: ionic balance; SAR: sodium adsorption ratio by Richards [26]; MAR: magnesium adsorption ratio by Raghunath [27]; %Na: sodium percentage by Todd and Mays [28]; RSBC: residual sodium bicarbonate by Gupta and Gupta [29]; PI: permeability index by Ragunath [27].

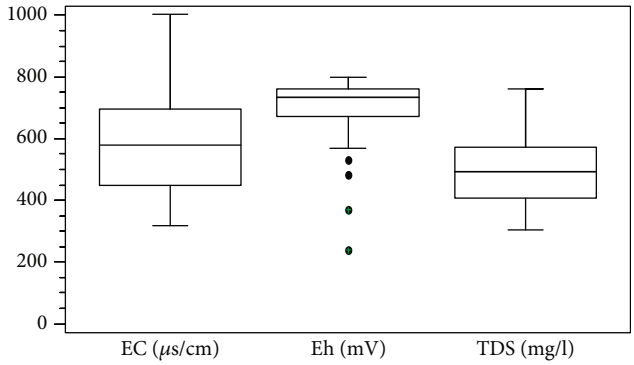

Figure 2: Box-and-whisker plots of physico-chemical parameters.

polyethylene bottles (50 and 100 ml). The bottles were filled to the top with water, capped without leaving any headspace, stored in a refrigerated container (about 4°C) during transportation to the laboratory, and then kept cool until analysis. At each sampling point, one water sample (for cation and trace elements) was collected and acidified in situ with suprapure HNO_3; a second filtered nonacidified sample was collected for anion analysis. Major anions (Cl^-, NO_3^-, NO_2^-, and SO_4^{2-}) and cations (Na^+, K^+, Mg^{2+}, and Ca^{2+}) were determined by ionic chromatography. Minor and trace elements (Li, B, Rb, Sr, Ba, V, and Cu) were determined by inductively coupled plasma–optical emission spectroscopy (ICP-OES). All trace element determinations were performed with the external standard calibration method, using NIST and SLRS standard reference materials for calibration. The precision of the analytical results was estimated by running triplicate analyses every ten samples. Uncertainty of measurements was ≤5-7% for all trace elements. Dissolved SiO_2 was measured by VIS spectrophotometry upon reaction with ammonium molybdate in acid media (and treatment with oxalic acid) to form a yellow silicomolybdate complex, whose absorbance was read at 410 nm [23]. Major element analyses were performed at the Analytical Chemical laboratory of the University of Basilicata; trace elements were determined using a Thermo Scientific™ iCAP™ 7200 at Gaudianello Company laboratory. The oxygen and hydrogen isotopic compositions were analysed at National Institute of Geophysical and Volcanology (INGV, Palermo, Italy) on unfiltered water samples using Analytical Precision AP 2003 and Finnigan MAT Delta Plus IRMS devices, respectively. The isotopic ratios are expressed as the deviation per mil (δ‰) from the reference V-SMOW. The uncertainties 1σ were ±0.1% for $\delta^{18}O$ and ±1% for δD.

3.2. Geochemical Modeling. The Geochemist's Workbench software (GWB 8.0, [24]), implemented with the Thermoddem database [25], was used to calculate saturation indices (SI) for the main mineral phases presents in the aquifer and the construction of activity diagrams. Saturation indices (SI) are defined as SI = log (IAP/Kt), where IAP is the ion activity product of the mineral–water reaction and Kt is the thermodynamic equilibrium constant at the measured temperature. Thus, SI = 0 indicates a thermodynamic equilibrium state, and values > 0 denote oversaturation and <0 undersaturation.

3.3. Irrigation Quality Parameters. In order to determine the suitability of the investigated groundwater for irrigation purposes, the following parameters were evaluated:

(i) The sodium adsorption ratio (SAR), by Richards [26]:

$$\mathrm{SAR} = \frac{\mathrm{Na}^+}{\sqrt{\mathrm{Ca}^{2+} + \mathrm{Mg}^{2+}/2}} \quad (1)$$

(ii) The magnesium adsorption ratio (MAR), by Raghunath [27]:

$$\mathrm{MAR} = \frac{\mathrm{Mg}^{2+}}{\left(\mathrm{Ca}^{2+}\mathrm{Mg}^{2+}\right)} * 100 \quad (2)$$

(iii) The sodium percentage (%Na), by Todd and Mays [28]:

$$\%\mathrm{Na} = \frac{\left(\mathrm{Na}^+ + \mathrm{K}^+\right)}{\left(\mathrm{Ca}^{2+} + \mathrm{Mg}^{2+} + \mathrm{Na}^+ + \mathrm{K}^+\right.} * 100 \quad (3)$$

(iv) The residual sodium bicarbonate (RSBC), by Gupta and Gupta [29]:

$$\mathrm{RSCB} = \left(\mathrm{HCO3}^- - \mathrm{Ca}^{2+}\right) \quad (4)$$

(v) The permeability index (PI), by Raghunath [27]:

$$\mathrm{PI} = \frac{\left(\mathrm{Na}^+ + \sqrt{\mathrm{HCO3}^-}\right)}{\left(\mathrm{Ca}^{2+} + \mathrm{Mg}^{2+} + \mathrm{Na}^+\right)} * 100 \quad (5)$$

where concentrations are expressed in meq/l.

4. Results

Temperature, pH, EC, Eh, and the total dissolved solids (hereafter TDS) and major elements are listed in Table 1 together with the geographical coordinates of the sampling points. The EC, Eh, and TDS box-and-whisker plots are shown in Figure 2. Temperatures were between 11 and 22.7°C, and overall water samples had nearly neutral pH-values. EC values ranged from 317 to 1000 μS/cm (average 583 ± 179 μS/cm). Eh values were positive (average 679 ± 142 mV). Finally, TDS ranged from 302 mg/l to 812 mg/l (average 502 ± 139 mg/l).

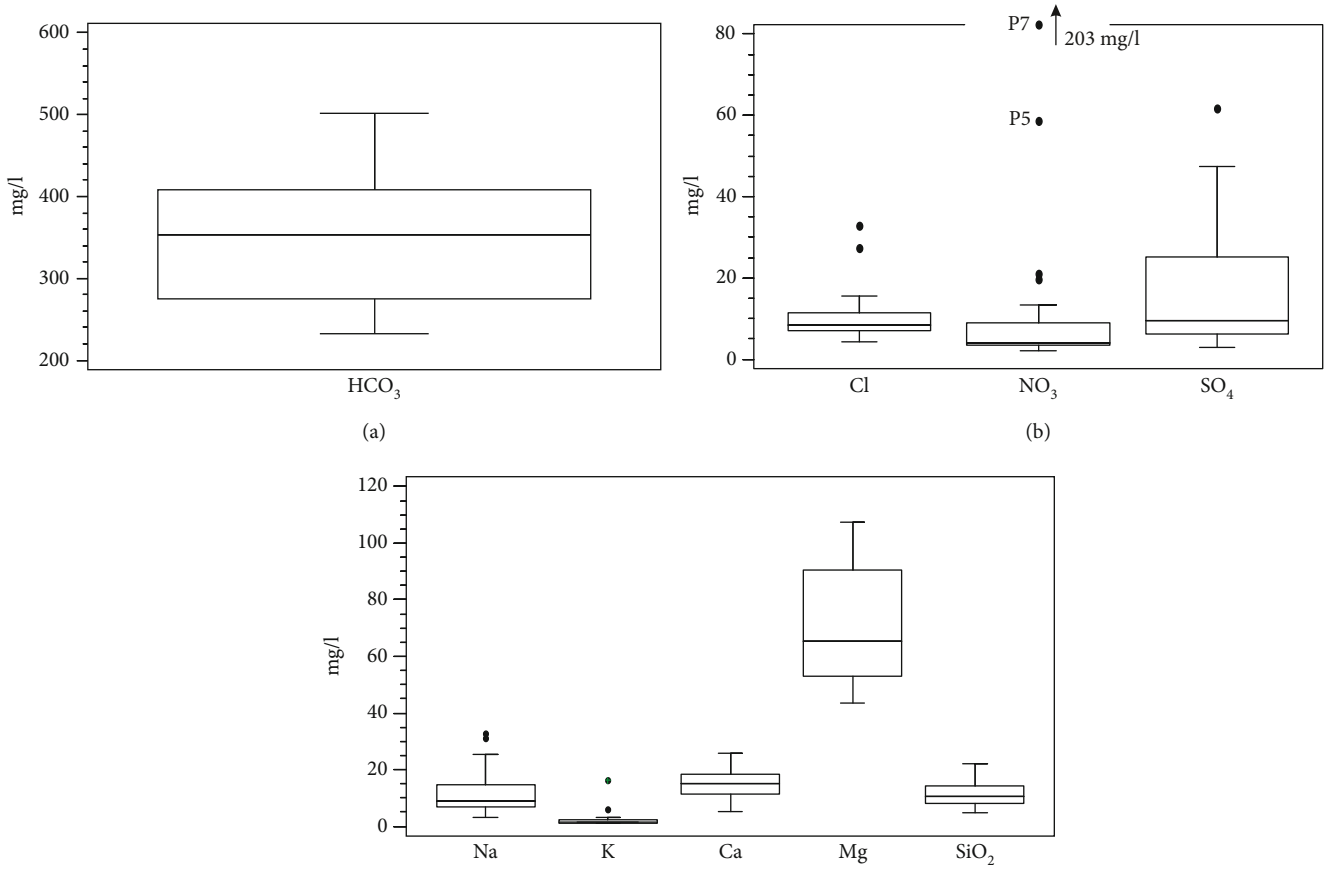

Figure 3: Box-and-whisker plots for major elements (cations and anions).

Box-and-whisker plots of the major constituents (cations and anions) are given in Figure 3.

Sulphates and magnesium count the greatest concentration variations. Among cations, Mg^{2+} is the most abundant (average 70.6 ± 20.6 mg/l), followed by Ca^{2+} (average 15 ± 5.1 mg/l), Na^{+} (11.3 ± 7.5 mg/l), and SiO_2 (11.1 ± 4.5 mg/l). K^{+} values are generally low, ranging from below instrumental detection limit (1.0 mg/l) to 3.2 mg/l, except for P7 sample having the highest value (16.5 mg/l). Bicarbonate is the main anion in solution with concentrations ranging between 232 and 502 mg/l, with an average value of 351.2 ± 86.5 mg/l. Sulphate contents are highly variable and range between 2.8 and 61.7 mg/l with an average value of 17.5 ± 16.6 mg/l. Cl^{-} concentrations are low with an average value of 10.3 ± 6.6 mg/l. Most of the investigated water samples have low NO_3^{-} contents ranging from below instrumental detection limit (1.9 mg/l) to 13.4 mg/l. Only 4 water samples, belonging to shallow porous aquifer, are outliers with NO_3 values ranging between 19.6 and 203 mg/l (P20, P8, P5, and P7 samples, respectively) (Figure 3). Trace element concentrations (Li, B, Rb, Sr, Ba, V, and Cu) are provided in Table 2, together with isotopic data and saturation indices of calcite, dolomite, anorthite, and albite.

V and Cu are characterized by very low contents and in many cases are below the detection limit (b.d.l.: 0.2 and 0.4 μg/l, respectively). Consequently, these elements will not be further included and treated in the discussion. Li and Rb are detected in most samples with values between b.d.l. and 21.2 μg/l and b.d.l. and 4.2 μg/l, respectively. Sr, B, and Ba are detected in all samples. Sr shows the greatest concentration variations from 35.2 to 593.6 μg/l, and some outliers are observed (Figure 4). B concentrations are from 3.8 to 66.1 μg/l while Ba values range from 4.9 to 123 μg/l.

Based on the Piper diagram, the investigated waters show a homogenous distribution with bicarbonate alkaline-earth composition (Figure 5).

Another useful index for water classification is Ionic Salinity or Total Ionic Salinity (TIS) that shows the sum of anion and cation total, expressed in meq/l [30]. Iso-TIS lines are reported in Figure 6 (SO_4^{2-} vs. $HCO_3^{-} + Cl^{-}$) where HAV waters falling in the 8 to 20 meq/l range because of their similar features.

The investigated waters showed $\delta^{18}O$ values between -7.2 and -8.9 ‰ and those of δD from -44 to -53 ‰. The waters from the karst and fissured aquifers generally showed more negative isotopic values (down to −8.9 and−53‰) than waters hosted by shallow porous aquifers, the latter displaying a wide range of variation, from −8.5 to −7.2‰ and from −44 to−52‰ for $\delta^{18}O$ and $\delta^{2}H$, respectively.

5. Discussion

5.1. Interelemental Relationships and Geochemical Processes. A *R*-mode factor analysis was performed to evaluate interelement relationships among some chemical-physical parameters (T and pH), major ions (Na^{+}, Ca^{2+}, Mg^{2+}, SO_4^{2-}, HCO_3^{-}), and

Table 2: Concentrations of selected minor elements, isotopic data, and saturation index (SI) in HAV groundwaters.

Sample	Li μg/l	B μg/l	Rb μg/l	Sr μg/l	Ba μg/l	V μg/l	Cu μg/l	δ^{18}O ‰ vs. V-SMOW	δD ‰ vs. V-SMOW	SI-calcite Log Q/K	SI-dolomite Log Q/K	SI-albite Log Q/K	SI-anortite Log Q/K
P1	1.9	10.5	b.d.l.	433	20.3	b.d.l.	1.2	-8.1	-46	-1.7	-1.0	-3.9	-11.1
P2	0.9	16.0	0.2	289	9.1	b.d.l.	b.d.l.	-8.3	-49	-1.1	-0.3	-1.7	-6.9
P4	b.d.l.	25.5	0.3	267	10.7	b.d.l.	0.4	-8.4	-52	-1.1	-0.2	-3.5	-10.4
P5	6.0	44.2	0.9	567	15.8	0.4	6.9	-7.8	-44	-0.9	0.0	-2.6	-10.0
P6	1.1	32.1	0.6	351	13.5	0.4	4.2	-8.0	-47	-1.0	0.0	-3.2	-10.3
P7	2.4	41.7	4.2	594	34.5	2.8	10.8	-8.4	-49	-0.7	0.3	-2.4	-9.6
P8	3.4	17.3	b.d.l.	245	37.8	0.2	0.4	-7.2	-46	-1.0	-0.1	-2.7	-9.8
P10	6.7	32.8	0.5	225	34.1	0.4	b.d.l.	-8.1	-51	-1.2	-0.6	-0.4	-5.3
P17	8.7	22.8	0.3	194	19.6	b.d.l.	2.6	-7.9	-47	-0.8	0.1	-2.9	-9.8
P18	2.1	17.4	2.0	367	20.8	b.d.l.	b.d.l.	-7.9	-48	-1.6	-1.4	-2.1	-10.1
P19	b.d.l.	15.6	0.3	204	18.7	b.d.l.	1.8	-8.0	-47	-1.6	-0.1	-4.1	-10.5
P20	b.d.l.	17.7	1.9	74	27.0	0.3	b.d.l.	-7.9	-48	-0.5	-1.6	-3.8	-10.6
P22	5.9	54.3	0.2	278	33.9	b.d.l.	1.7	-7.7	-46	-0.6	0.5	-2.7	-9.7
P23	2.9	33.9	0.5	490	89	b.d.l.	1.8	-7.8	-46	-1.0	0.4	-3.5	-10.0
P24	3.2	42.2	b.d.l.	379	123	b.d.l.	0.1	-8.5	-50	-0.8	-0.2	0.4	-4.1
S3	2.4	15.6	0.9	265	10.3	0.4	1.5	-8.9	-53	-0.8	0.3	-4.1	-10.6
S11	b.d.l.	4.7	0.8	43	6.8	1.0	b.d.l.	-8.7	-50	-1.1	0.0	-4.3	-10.4
S12	b.d.l.	b.d.l.	0.4	35	4.9	1.0	b.d.l.	-8.7	-51	-1.0	-0.5	-4.3	-10.6
S13	b.d.l.	3.8	1.1	54	8.2	0.6	b.d.l.	-8.9	-53	-0.9	-0.4	-3.9	-10.3
S14	b.d.l.	5.8	1.0	49	8.3	1.2	b.d.l.	-8.3	-49	-0.9	-0.3	-2.6	-7.4
S15	2.0	19.5	1.0	147	18.9	1.2	3.9	-7.9	-47	-0.8	-0.3	-3.4	-10.1
S16	1.3	13.9	0.8	123	15.4	1.3	0.4	-8.1	-47	-0.9	0.1	-3.7	-10.1
S21	21.2	66.1	1.0	204	45	b.d.l.	b.d.l.	-8.2	-48	-1.1	-0.7	-2.9	-10.0
S25	3.3	22.9	0.9	234	23.4	0.4	b.d.l.	-8.0	-49	-1.2	-0.8	-3.0	-10.1
d.l.	1.0	5.0	0.2	10.0	2.0	0.2	0.4						

d.l.: detection limit; b.d.l.: below detection limit.

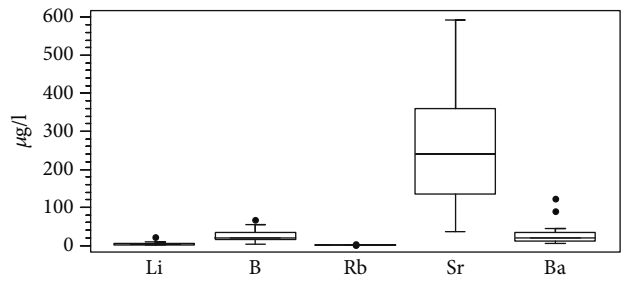

Figure 4: Box-and-whisker plot of selected trace elements.

selected trace elements (Sr, Ba, B). Factors were extracted after varimax rotation using the STATGRAPHICS 18 package. This operation was performed using a standardized correlation matrix, classical type of factoring, thereby equally weighting all the variables during factor calculations. The communalities provide an index of the efficiency of the proposed set of factors [31], and the magnitude of the communalities calculated in this study suggests that most of the original variance is still accounted for by the present set of factors. Three factors explain 94% of the total variance in the selected database (Table 3).

Usually, in terrains where the carbonate lithological facies is dominated by the occurrence of dolomite, the bicarbonate alkaline-earth hydrofacies, with higher Mg^{2+} values than Ca^{2+} one, can be ascribed to dolomite dissolution. It is well known that the dissolution of dolomite can be expressed as follows:

$$CaMg(CO_3)_2 + 2H_2O + 2CO_2 \longrightarrow Ca^{2+} + Mg^{2+} + 4HCO_3^- \quad (6)$$

and the water-dolomite interaction should release equally charged amounts of $Ca^{2+} + Mg^{2+}$ and HCO_3^-, with a $(Ca^{2+} + Mg^{2+}/HCO_3^-)$ ratio close to 1.

Accordingly, in our case, the correlation between $(Ca^{2+}+Mg^{2+}$and $HCO_3^-)$ is highly significant ($r = 0.86$, p value < 0.001, Figure 7). Only P7 sample falls away from general trend, maybe because of its anthropogenic component (see discussion below). However, both the $(Ca^{2+}+Mg^{2+}/HCO_3^-)$ and Mg^{2+}/Ca^{2+} ratios, as meq/l, are above 1, claiming for additional source(s) of Mg^{2+} in groundwater, as also suggested by the finding that several samples are oversaturated with respect to dolomite or close to the SI = 0 value (Table 2, Figure 8).

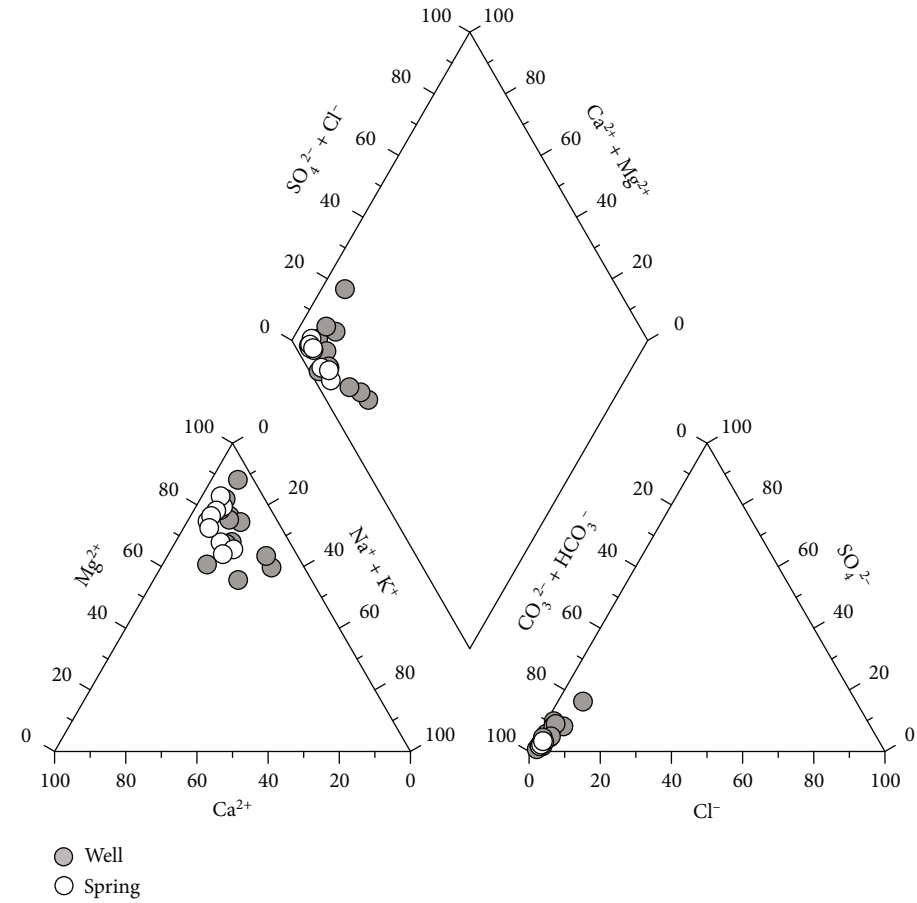

Figure 5: Piper diagram.

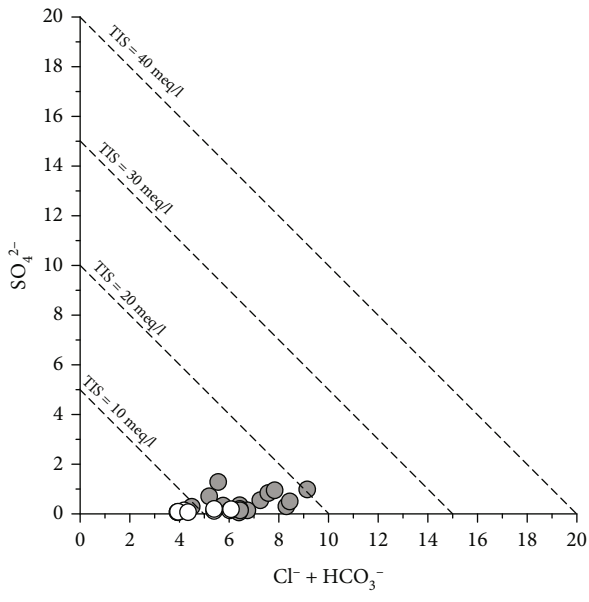

Figure 6: Correlation diagram of SO_4^{2-} vs. $HCO_3^- + Cl^-$ for the water samples. The symbols are as Figure 5.

The correlation between dissolved silica and Mg^{2+} is significant ($r = 0.65$, $p < 0.01$), clearly indicating silicate dissolution as additional source of Mg^{2+} in solution. The incongruent dissolution of silicates reacting with CO_2 derived from microorganism respiration and/or mineralization of soil organic matter can promote a Mg^{2+} surplus into the groundwater [32] and references therein. F1 thus represents the combined effect of dolomite and silicate dissolution on the release of Mg^{2+} in solution.

The second factor (F2; var.% = 15.2) includes significant and positive weightings for the largely soluble ions Na^+, Cl^-, and SO_4^{2-}. Overall, the investigated waters have Na/Cl meq/l ratio > 1, suggesting that Na^+ in groundwater may derive from weathering of mineral phases different from the common NaCl salt. The positive correlation between dissolved silica and Na^+($r = 0.66$, $p < 0.01$) associated with negative values of the feldspars SI (albite and anorthite, Table 2) suggests that the silicate incongruent dissolution is ongoing process allowing the release of Na^+ in solution.

Further, the log a $(H_4SiO_4)_{aq}$ vs. log a (Na^+/H^+) activity diagram (Figure 9) shows that the studied waters are in equilibrium with kaolinite, a T-O clayey mineral with a minor cation exchange capacity with respect to other clays, that does not include in its lattice interlayered cations such as Na^+. This, in turn, means that kaolinite cannot contribute to narrow down the Na^+ content in HAV groundwater. As

Table 3: Matrix of factor weights after varimax rotation using the STATGRAPHICS 18 package.

	Factor 1	Factor 2	Factor 3
T (°C)			
pH			
Na^+ (mg/l)		0.68	
Ca^{2+} (mg/l)			
Mg^{2+} (mg/l)	0.83		
HCO_3^-(mg/l)	0.92		
Cl^- (mg/l)		0.88	
SO_4^{2-}(mg/l)		0.85	
B (μg/l)			0.88
Sr (μg/l)			
Ba (μg/l)			
Total variance (%)	67.6	15.2	11.2
Cumulative variance (%)	67.6	82.8	94

Numbers are weights of the variables in the extracted factors. Variables having weights < 0.65 are omitted.

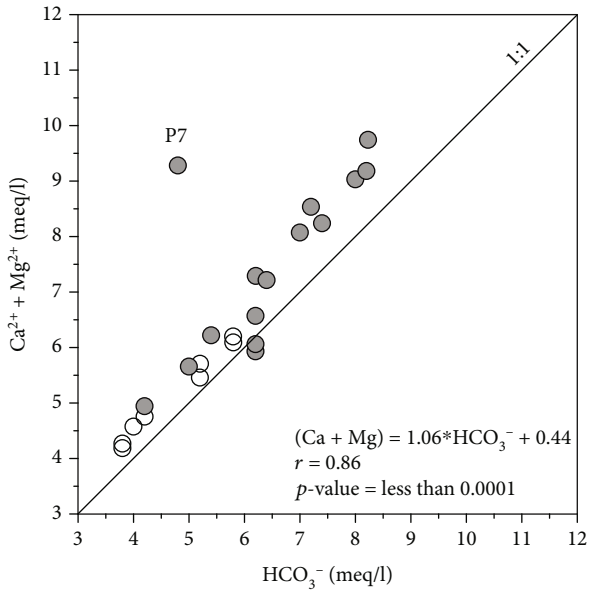

Figure 7: Binary plot of Ca^{2+} + Mg^{2+} vs. HCO_3^- concentrations. The symbols are as Figure 5.

for Cl^-, its geogenic abundance in groundwater increases with groundwater age [33], and excluding salt dissolution and marine spray supply at inland [34] and references therein, Cl^- may mostly derive from anions exchange at the clay mineral edges. In fact, depending on the pH of solution and due to protonation reactions at the broken bonds of both octahedral and tetrahedral layers, the clay mineral edges may be positively charged, promoting anions adsorption, e.g., [35].

The likely lack of sulphate minerals (anhydrite and gypsum) in HAV lithologies excludes a SO_4^{2-} origin through salt solubilization. Although oxidative reaction affecting suphides (e.g., pyrite FeS_2) dispersed in rocks, even in small amounts, may represent a source for SO_4^{2-} in groundwater, the use of

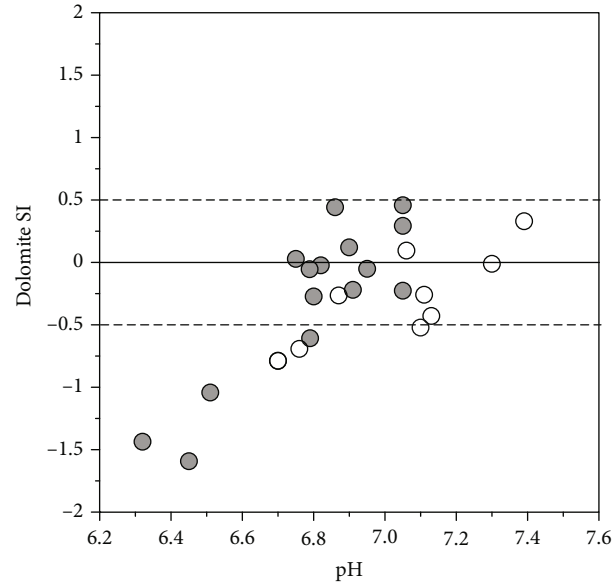

Figure 8: Diagram of the saturation indexes of dolomite (SI) and the pH values. The symbols are as Figure 5.

N-rich fertilizers may also originate most of the SO_4^{2-} in solution from the recycling of the groundwater used in irrigation. As shown in Figure 10 (NO_3^- vs. SO_4^{2-}), two different trends are clearly recognized. In the first one, involving exclusively well waters (except for S25 sample), the NO_3^-/SO_4^{2-} ratio is close to 1, and NO_3^- contents are generally >4 mg/l. P5 and P7 samples have the highest NO_3^- and SO_4^{2-} values. Although there are no baseline data on the NO_3^- geogenic level in the area, it is known that nitrate concentrations above 4 mg/l can be referred to anthropogenic contamination, e.g., [36, 37]. In our case, this supports the idea of an anthropogenic origin for SO_4^{2-}, mostly due to agriculture fertilizers. The second trend is outlined by a few wells showing larger SO_4^{2-} contents and low NO_3^- contents and suggests a possible geogenic origin for SO_4^{2-} due to oxidative reaction affecting suphides.

In the third factor (F3; var.% = 11.2), only boron has a significant weight. Boron contents in groundwater may be affected by anthropogenic activities [38] and interaction with evaporite levels, e.g., [39] and references therein. In the aqueous environment, B is a very mobile element occurring as boric acid ($B(OH)_3$) in dilute aqueous solution at pH < 7 and as prevailing metaborate anion ($B(OH)_4^-$)at pH > 10, e.g., [40] and references therein. Boron may have several possible natural and anthropogenic sources in inland aquifers including, for instance, leaching of geologic materials as well as domestic wastewater, e.g., [41] and references therein. The low B concentration observed in the HAV groundwater (well below 100 μg/l) appears to exclude any significant anthropogenic source. F3 thus likely accounts for the solubilization of B by leaching of sedimentary deposits of marine and non-marine origin, e.g., [42] and references therein.

5.2. Isotopic Constraints. Water isotopes are used to define water origin, recharge areas, circulation paths, and mixing or exchange processes [43–45]. The δD and δ^{18}O values are displayed in Figure 11, together with the Northern Calabria

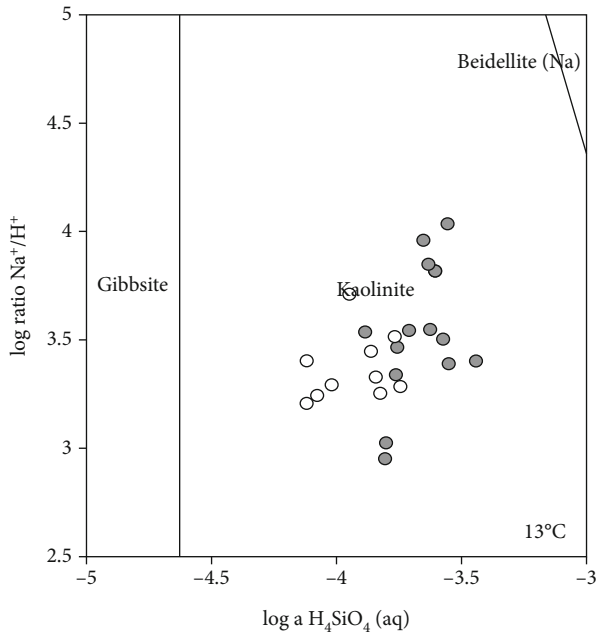

Figure 9: Activity plot of log a (H_4SiO_4) vs. log a (Na^+/H^+). The symbols are as Figure 5.

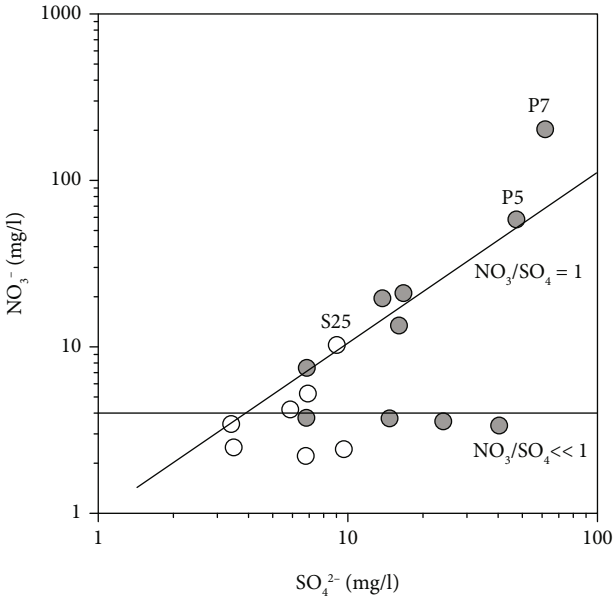

Figure 10: Relationships between SO_4^{2-} and NO_3^- contents in HAV water samples. The water samples with NO_3^- values lower than detection limit (1.9 mg/l) are not reported. P5 and P7 water samples have higher NO_3^- values. The NO_3^- geogenic level (equal to 4 mg/l) has been drawn. The symbols are as Figure 5.

Meteoric Water Line (NCMWL: $6.22 * \delta^{18}O + 5.21$ [46]), the Southern Italy Meteoric Water Line (SIMWL: $6.7 * \delta^{18}O + 5.2$ [47]), and the Global Meteoric Water Line (GMWL: $\delta D = 8.17 * \delta^{18}O + 10.35$ [48]). Spring waters are well-correlated ($r = 0.95$, p value < 0.0001, Figure 11(a)) and fall between SIMWL and NCMWL, while well waters show a wider data distribution ($r = 0.66$, p value = 0.013, Figure 11(b)) falling between GMWL and NCMWL. Both water types are fed by rainwater and have a meteoric origin.

The isotope data variation, measured in well waters, is probably linked to seasonal rainfall effect since the shallow porous aquifer has a relatively short and surface hydrogeological circuits through the gravelly-sandy permeable deposits of the quaternary succession.

Spring waters from karst and fissured aquifers showing a narrow range of O and ^2H isotopic values can be used to deduce the mean elevation of the recharge area through the equation proposed for southern Italy by Vespasiano et al. [46]:

$$\delta^{18}O = -0.00194 \times Hi - 5.91, \quad (7)$$

and a range of 1030 to 1540 meter a.s.l mean elevation of the recharge areas has been estimated. The inferred range is consistent with the elevation of the springs located in the highly fissured limestones (Carbonate Platform) and in the underlying "Calcari con Selce" Fm (Lagonegro Units). In addition, S11, S12, and S13 springs with more negative isotope data have longer and deeper hydrogeological circuit likely due to the local geological complexity affecting the recharge area to the west and north-west [17].

5.3. Groundwater for Irrigation and Drinking Uses. The groundwater quality is of fundamental relevance for irrigation and drinking purposes [3], also in the northern bank of the Mediterranean, affected by climate change evolving toward semiarid to arid conditions, e.g., [49] and references therein. The amount of dissolved ions affects the agricultural productivity influencing both the growth of plants and soil structure [50]. Some important irrigation quality parameters (such as SAR, MAR, %Na, RSBC, and PI) are largely used for determining the suitability of groundwater for a proper agricultural uses [8, 51, 52] and references therein. Irrigation water quality parameters of the analysed groundwater are shown in Table 1.

The %Na vs. EC plot [53] provides a mostly adopted method for rating irrigation water. In Figure 12, the HAV groundwater falls in the "excellent to good" and to a lesser extent in the "good to permissible" fields. Similarly, the PI indicates that the HAV groundwater is suitable for irrigation, being ranked as class I (PI: 30-50%; total concentration: 13-39 meq/l). However, in the SAR vs. EC diagram [26], the HAV groundwater is ranked as C2S1 and C3S1 (medium to high salinity hazard and low sodium hazard, Figure 12).

Excess salinity reduces the osmotic activity of plants limiting the absorption of water and nutrients from the soil of exchange able sodium, e.g., [54]. This suggests that efforts, including leaching and proper drainage, are needed in order to control the salinity hazard, especially for those waters, representing a significant part of HAV groundwater dataset, having EC higher than 750 μs/cm.

Accordingly, some concerns also arise from the RSBC values, mostly related to the relatively high HCO_3^- content, that in most samples is >5 meq/l, implying that HAV

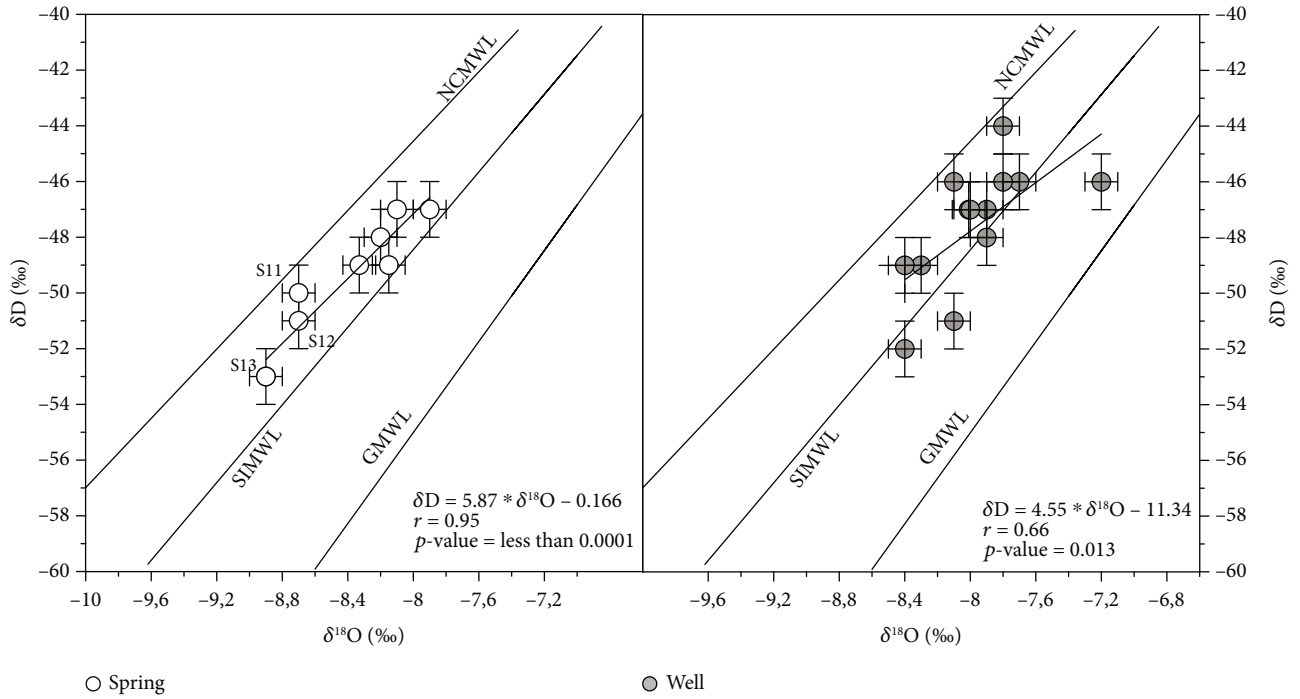

Figure 11: $\delta^{18}O$ and δD of the groundwater samples, as compared with meteoric water lines (Northern Calabria Meteoric Water Line (NCMWL), $6.22 * \delta^{18}O + 5.21$, [46]; Southern Italy Meteoric Water Line (SIMWL), $6.7 * \delta^{18}O + 5.2$, [47]; Global Meteoric Water Line (GMWL), $\delta D = 8.17 * \delta^{18}O + 10.35$, [48]).The uncertainties 1σ (±0.1% for $\delta^{18}O$ and ±1% for δD) were reported.

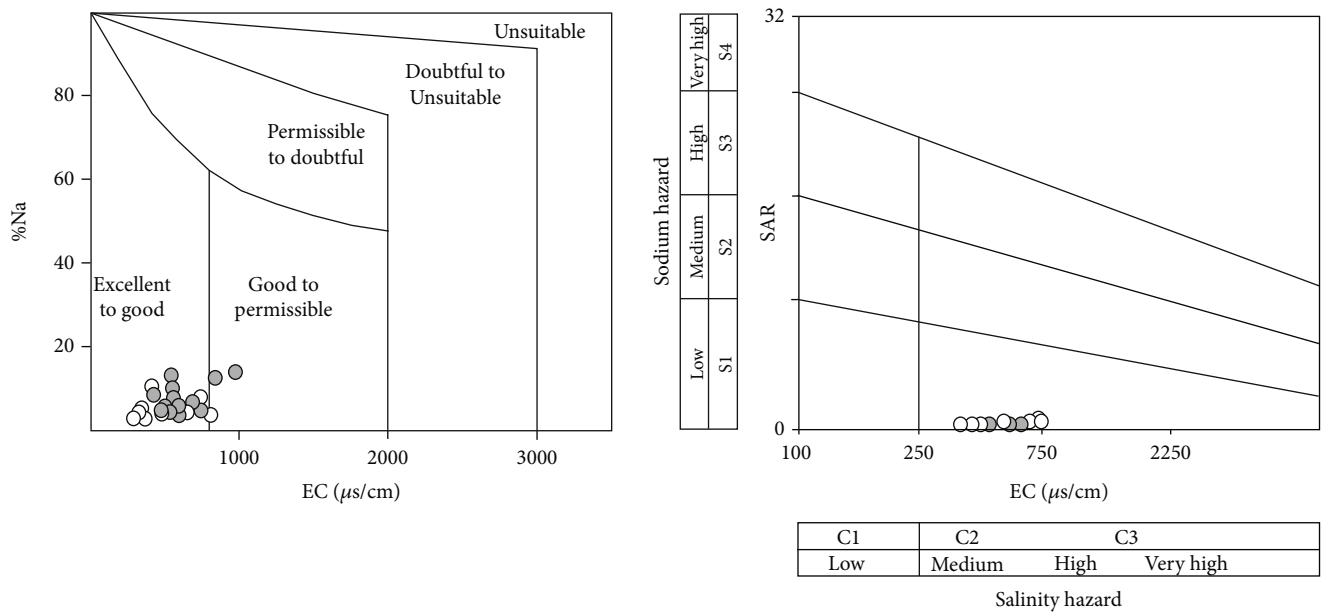

Figure 12: Plots of calculated values of %Na and SAR vs. EC of groundwater samples (after Wilcox [53] and [26], respectively). The symbols are as Figure 5.

groundwater cannot be classified as fully satisfactory for irrigation purposes according to Gupta and Gupta [29]. RSBC exceeding 5 meq/l may cause an alkalizing effect, claiming for a bicarbonate neutralization when long-term irrigation purposes are required [55]. An additional alkalizing effect is also due to high Mg^{2+} contents in groundwater. Usually, Ca^{2+} and Mg^{2+} are in equilibrium in most waters, and Raghunath [27] and Gupta and Gupta [29] suggested that MAR values exceeding 50% indicate magnesium hazard as soils become more alkaline [56], favoring the decrease of phosphorous availability [57]. In the HAV groundwater, MAR is always >70% indicating magnesium hazard and suggesting long-term magnesium monitoring in the area in order to plan alkalinity mitigation policies.

Table 4: Drinking water quality standard of WHO [60] and Italian legislation (D. Lgs. 31/2001, [58]).

Parameter/element	WHO (2004)		D. Lgs. 31/2001
	Desirable limit (DL)	Maximum permissible limit (MPL)	Maximum admissible concentrations (MAC)
pH	7-8.5	9	-
EC (μS/cm)	500	1500	-
TDS (mg/l)	500	1500	-
Cl^- (mg/l)	200	600	250
SO_4^{2-} (mg/l)	200	400	250
HCO_3^- (mg/l)	-	240	-
NO_3^- (mg/l)	-	50	50
NO_2^- (mg/l)	-	3	0.5
Ca^{2+} (mg/l)	75	200	-
Mg^{2+} (mg/l)	50	150	-
Na^+ (mg/l)	-	200	200
K^+ (mg/l)	-	12.0	-
Cu (mg/l)	-	1.0	1.0
Ba (mg/l)	-	2.0	-
B (mg/l)	-	0.5	1.0
Sr (mg/l)	-	0.5	-
V (mg/l)	-	-	0.05

-: no data.

In Italy, groundwater quality for drinking use is regulated by D. Lgs 31/2001 [58] (acceptance of the 98/83/EU directive [59]) which provides for the measurement of indicator parameters (such as odor, color, taste, pH, and hardness) and chemical and microbiological parameters. In this study, a preliminary assessment of groundwater quality for drinking use was proposed considering only some indicator and chemical parameters analysed. The drinking water quality was compared with the conditions set by the World Health Organization 2004 (hereafter WHO 2004 [60]) and the Italian legislation (D. Lgs. 31/2001). The relative maximum admissible concentrations (hereafter MAC) imposed for protecting of groundwater resources by the Italian legislation [58], and the desirable limit (DL) and maximum permissible limit (MPL) prescribed by WHO for drinking purposes are shown in Table 4.

Most water samples have TDS below DL of 500 mg/l as defined by the WHO, and overall HAV groundwater has TDS below MPL of 1500 mg/l as defined by the WHO specification for drinking water. In most samples, HCO_3^- exceeds the MPL defined by the WHO (240 mg/l). Na^+, Cl^-, and SO_4^{2-} are below the respective MPL (Na^+ = 200 mg/l; Cl^- = 600 mg/l; SO_4^{2-} = 400 mg/l).

NO_3^- contents are always below the MAC of 50 mg/l except for two water samples (P5 and P7) having very high NO_3^- values (58 and 203 mg/l, respectively). Some environmentally relevant trace elements, including B, V, and Cu, are characterized by very low contents, below the respective MAC and MPL. Ba and B are below the guideline values provided by the WHO for drinking water whereas Sr^{2+} exceeds the MPL (0.5 mg/l) in two water samples (P5 and P7). Our data allows to state that P5 and P7 water samples, used only for irrigation use, show critical issue for Sr^{2+} and NO_3^- concentrations. As previously said, high NO_3^- values are well-related to SO_4^{2-} contents and are linked to human activities, including mainly agricultural activities.

As to strontium values, it is well known that Sr-bearing minerals (mainly carbonate and sulphate) are distributed in a number of rock types, and Sr^{2+} release from minerals and rocks to water by weathering processes is very common [61]. Strontium, in fact, readily reacts with water and oxygen to form insoluble mineral phases or create complexes with carbonate and silicate depending on the water mineralization. Therefore, high Sr^{2+} concentrations may indicate an anthropogenic input by agricultural activities such as the use of fertilizers, carbonate additives, manure (i.e., cattle and poultry) and dumping, and industrial wastes [62]. Excluding P5 and P7 samples, a good and positive correlation between Sr^{2+} and HCO_3^- is evident for the analysed dataset ($r = 0.75$, $p < 0.01$), suggesting that Sr^{2+} contents are linked to carbonate phases. Conversely, as P5 and P7 waters show high NO_3^- and SO_4^{2-} contents, in addition to the Sr^{2+} ones, a contribution from agricultural practices cannot be excluded for these waters. Although a microbiological characterization is required for defining the overall groundwater quality, based on the analysed inorganic component, all HAV groundwaters are suitable for drinking use, except for two well waters.

6. Conclusions

Groundwater is an essential water resource for drinking and irrigation uses in the HAV. In this study, hydrogeochemistry coupled with multivariate statistics, saturation indices, and stable isotope composition was used to assess the geochemical processes controlling the groundwater chemistry. Consequently, groundwater quality and its suitability for drinking and agricultural use were evaluated. All the examined groundwater has a meteoric origin although some springs show long and deep flow than the other ones. The main geochemical process affecting water chemistry is the dolomite and silicate dissolution that is also controlled by the concentration and distribution of trace elements. The SO_4^{2-}/NO_3^- ratios suggest that an anthropogenic contamination, mostly associated with the use of agriculture fertilizers, cannot be excluded for some water samples (P5 and P7 samples). The suitability of water for drinking purposes was evaluated by comparing different chemical parameters with those reported by the World Health Organization [29] and the Italian legislation guidelines. Our results demonstrate that most of HAV groundwater is chemically suitable for drinking use with respect to the analysed inorganic chemical elements. As to agricultural use, the % Na and PI indicate that groundwater is generally useful for irrigation, although SAR, MAR, and RSBC highlight a medium to high salinity hazard. In light of the recent increase in human activities (i.e., industrialization and intensive agricultural practices), this study represents a warning for the local authorities providing significant insights to delineate a successful policy for management of groundwater resources.

Data Availability

The data used to support the findings of this study are included within the article.

Disclosure

Part of the paper is related to Maria Assunta Musto Master degree thesis (University of Basilicata, Potenza-Italy).

Conflicts of Interest

There are no conflicts of interest to declare.

Authors' Contributions

All the authors have approved the manuscript and agree with submission to your esteemed journal.

Acknowledgments

The authors are indebted to Prof. ssa Giuliana Bianco and Dr. Raffaella Pascale for their support during chemical analysis at University of Basilicata. This research has been supported by a grant (RIL2009-Unibas) of G. Mongelli and M. Paternoster and partially by the project "Detection and tracking of crustal fluid by multi-parametric methodolo-gies and technologies" of the Italian PRIN-MIUR programme (grant no. 20174X3P29).

References

[1] X. Wang, L. Zhang, Z. Zhao, and Y. Cai, "Heavy metal pollution in reservoirs in the hilly area of southern China: distribution, source apportionment and health risk assessment," *Sci. Total Environ.*, vol. 634, pp. 158–169, 2018.

[2] S. Melki, E. L. Mabrouk, A. Asmi, M. O. B. Sy, and M. Gueddari, "A geochemical assessment and modeling of industrial groundwater contamination by orthophosphate and fluoride in the Gabes-North aquifer, Tunisia," *Environmental Earth Sciences*, vol. 79, no. 6, 2020.

[3] S. Melki, E. L. Mabrouk, A. Asmi, and M. Gueddari, "Inferred industrial and agricultural activities impact on groundwater quality of Skhira coastal phreatic aquifer in Southeast of Tunisia (Mediterranean region)," *Geofluids*, vol. 2019, 19 pages, 2019.

[4] G. Vespasiano, G. Cianflone, C. B. Cannata, C. Apollaro, R. Dominici, and R. De Rosa, "Analysis of groundwater pollution in the Sant'Eufemia Plain Calabria–South Italy," *Italian Journal of Engineering Geology and Environment*, vol. 16, no. 2, pp. 5–15, 2016.

[5] G. Vespasiano, G. Cianflone, A. Romanazzi et al., "A multidisciplinary approach for sustainable management of a complex coastal plain: the case of Sibari Plain (Southern Italy)," *Marine and Petroleum Geology*, vol. 109, pp. 740–759, 2019.

[6] S. Parisi, M. Paternoster, F. Perri, and G. Mongelli, "Source and mobility of minor and trace elements in a volcanic aquifer system: Mt. Vulture (southern Italy)," *Journal of Geochemical Exploration*, vol. 110, no. 3, pp. 233–244, 2011.

[7] S. Muhammad, M. T. Shah, and S. Khan, "Health risk assessment of heavy metals and their source apportionment in drinking water of Kohistan region, northern Pakistan," *Microchemical Journal*, vol. 98, no. 2, pp. 334–343, 2011.

[8] M. B. Alaya, S. Saidi, T. Zemni, and F. Zargouni, "Suitability assessment of deep groundwater for drinking and irrigation use in the Djeffara aquifers (Northern Gabes, South-Eastern Tunisia)," *Environment and Earth Science*, vol. 71, no. 8, pp. 3387–3421, 2014.

[9] C. Apollaro, A. Caracausi, M. Paternoster et al., "Fluid geochemistry in a low-enthalpy geothermal field along a sector of southern Apennines chain (Italy)," *Journal of Geochemical Exploration*, vol. 219, p. 106618, 2020.

[10] M. Paternoster, G. Oggiano, R. Sinisi, A. Caracausi, and G. Mongelli, "Geochemistry of two contrasting deep fluids in the Sardinia microplate (western Mediterranean): relationships with tectonics and heat sources," *Journal of Volcanology and Geothermal Research*, vol. 336, pp. 108–117, 2017.

[11] R. Buccione, E. Fortunato, M. Paternoster et al., "Mineralogy and heavy metal assessment of the Pietra del Pertusillo reservoir sediments (Southern Italy)," *Environmental Science and Pollution Research*, vol. 28, no. 4, pp. 4857–4878, 2021.

[12] G. Cello, R. Gambini, S. Mazzoli, A. Read, E. Tondi, and V. Zucconi, "Fault zone characteristics and scaling properties of the Val d'Agri Fault System (southern Apennines, Italy)," *Journal of Geodynamics*, vol. 29, no. 3-5, pp. 293–307, 2000.

[13] E. Gueguen, M. Bentivenga, R. Colaiacovo, S. Margiotta, V. Summa, and I. Adurno, "The Verdesca landslide in the Agri Valley (Basilicata, Southern Italy): a new geological and geomorphological framework," *Natural Hazards and Earth System Sciences*, vol. 15, no. 11, pp. 2585–2595, 2015.

[14] M. Schiattarella, P. Di Leo, P. Beneduce, and S. I. Giano, "Quaternary uplift vs tectonic loading: a case study from the Lucanian Apennine, southern Italy," *Quaternary International*, vol. 101-102, pp. 239–251, 2003.

[15] A. Giocoli, T. A. Stabile, I. Adurno et al., "Geological and geophysical characterization of the southeastern side of the High Agri Valley (southern Apennines, Italy)," *Natural Hazards and Earth System Sciences*, vol. 15, no. 2, pp. 315–323, 2015.

[16] T. A. Stabile, A. Giocoli, V. Lapenna, A. Perrone, S. Piscitelli, and L. Telesca, "Evidence of low-magnitude continued reservoir-induced seismicity associated with the Pertusillo artificial lake (southern Italy)," *Bulletin of the Seismological Society of America*, vol. 104, no. 4, pp. 1820–1828, 2014.

[17] S. Carbone, S. Catalano, S. Lazzari, F. Lentini, and C. Monaco, "Presentazione della carta geologica del Bacino del Fiume Agri (Basilicata)," *Memorie della Società Geologica Italiana*, vol. 47, pp. 129–143, 1991.

[18] S. I. Giano, V. Lapenna, S. Piscitelli, and M. Schiattarella, "Electrical imaging and self-potential surveys to study the geological setting of the quaternary slope deposits in the Agri High Valley (southern Italy)," *Annali di Geofisica*, vol. 43, pp. 409–419, 2000.

[19] G. Spilotro, F. Caporale, F. Canora, M. Di Cagno, G. Leandro, and M. Moreno, "Idrodinamica della piana alluvionale dell'Alta Val d'Agri," in *Le risorse idriche sotterranee dell'Alta Val d'Agri*, A. Colella, Ed., Collana Editoriale di Studi e Ricerche dell'Autorità Interregionale di Bacino della Basilicata, n. 3, Potenza, 2003.

[20] M. Civita, M. De Maio, and B. Vigna, "Studio delle risorse sorgive degli acquiferi carbonatici dell'Alta Val D'Agri," in *Le risorse idriche sotterranee dell'Alta Val d'Agri*, A. Colella, Ed., Collana Editoriale di Studi e Ricerche dell'Autorità Interregionale di Bacino della Basilicata, n. 3, Potenza, 2003.

[21] A. Colella, V. Lapenna, and E. Rizzo, "La struttura sepolta del bacino dell'Alta Val d'Agri (Pleistocene, Basilicata)," in *Le risorse idriche sotterranee dell'Alta Val d'Agri*, A. Colella, Ed., Collana Editoriale di Studi e Ricerche dell'Autorità Interregionale di Bacino della Basilicata, n. 3, Potenza, 2003.

[22] M. Paternoster, A. Scarfiglieri, and G. Mongelli, "Groundwater chemistry in the high Agri Valley (southern Apennines, Italy)," *Geo Acta*, vol. 4, pp. 25–41, 2005.

[23] L. M. L. Nollet, *Handbook of Water Analysis*, CRC press, 2nd edition, 2000.

[24] C. M. Bethke, "The Geochemist's Workbench® Release 8.0 (four volumes)," in *Hydrogeology Program*, University of Illinois, Urbana, Illinois, 2010.

[25] P. Blanck, A. Lassin, P. Piantone et al., "Thermoddem: a geochemical database focused on low temperature water/rock interactions and waste materials," *Applied Geochemistry*, vol. 27, no. 10, pp. 2107–2116, 2012.

[26] L. A. Richards, "Diagnosis and Improvement of Saline Alkali Soils," in *Agriculture, vole 160. Handbook 60*, US Department of Agriculture, Washington, 1954.

[27] H. M. Raghunath, *Groundwater*, Wiley, New Delhi, 1987.

[28] D. K. Todd and L. W. Mays, *Groundwater Hydrology*, Wiley, New York, 3rd edition, 2005.

[29] S. K. Gupta and I. C. Gupta, *Management of Saline Soils and Water*, Oxford and IBM Publ. Co, New Delhi, 1987.

[30] C. Apollaro, V. Tripodi, G. Vespasiano et al., "Chemical, isotopic and geotectonic relations of the warm and cold waters of the Galatro and Antonimina thermal areas, southern Calabria, Italy," *Marine and Petroleum Geology*, vol. 109, pp. 469–483, 2019.

[31] J. C. Davis, *Statistics and Data Analysis in Geology. Vol. 646*, John Wiley & Sons, New York, 1986.

[32] F. Frondini, O. Vaselli, and M. Vetuschi Zuccolini, "Consumption of atmospheric carbon dioxide through weathering of ultramafic rocks in the Voltri Massif (Italy): quantification of the process and global implications," *Geosciences*, vol. 9, no. 6, p. 258, 2019.

[33] J. R. Degnan, B. D. Lindsey, J. P. Levitt, and Z. Szabo, "The relation of geogenic contaminants to groundwater age, aquifer hydrologic position, water type, and redox conditions in Atlantic and Gulf Coastal Plain aquifers, eastern and south-central USA," *Science of the Total Environment*, vol. 723, p. 137835, 2020.

[34] G. Mongelli, S. Monni, G. Oggiano, M. Paternoster, and R. Sinisi, "Tracing groundwater salinization processes in coastal aquifers: a hydrogeochemical and isotopic approach in the Na-Cl brackish waters of northwestern Sardinia, Italy," *Hydrology and Earth System Sciences*, vol. 17, no. 7, pp. 2917–2928, 2013.

[35] G. H. Bolt and M. G. M. Bruggenwert, *Soil Chemistry. A: Basic elements*, Elsevier, Amsterdam, Netherlands, 1978.

[36] I. S. Babiker, A. A. Mohamed, H. Terao, K. Kato, and K. Ohta, "Assessment of groundwater contamination by nitrate leaching from intensive vegetable cultivation using geographical information system," *Environment International*, vol. 29, no. 8, pp. 1009–1017, 2004.

[37] G. Mongelli, M. Paternoster, and R. Sinisi, "Assessing nitrate origin in a volcanic aquifer using a dual isotope approach," *International journal of Environmental Science and Technology*, vol. 10, no. 6, pp. 1149–1156, 2013.

[38] E. Giménez and I. Morell, "Utilisación del boro comoindicatoro de contaminacion en la Plana de Castellon," *Hidrogeologica y Recursos Hidraulicos XVI (IV)*, vol. 16, pp. 285–292, 1992.

[39] O. Hebrard, S. Pistre, N. Cheynet, J. Dazy, C. Batiot-Guilhe, and J. L. Seidel, "Origine des eaux des émergences karstiques chlorurées du Languedoc-Roussillon," *Comptes Rendus Geoscience*, vol. 338, no. 10, pp. 703–710, 2006.

[40] S. Cuccuru, F. Deluca, G. Mongelli, and G. Oggiano, "Granite and andesite-hosted thermal water: geochemistry and environmental issues in northern Sardinia, Italy," *Environmental Earth Sciences*, vol. 79, no. 11, p. 257, 2020.

[41] P. M. Buszka, J. Fitzpatrick, L. R. Watson, and R. T. Kay, "Evaluation of ground-water and boron sources by use of boron stable-isotope ratios, tritium, and selected water-chemistry constituents near Beverly Shores, Northwestern Indiana," *U.S. Geological Survey Scientific Investigations Report 2007–5166, U.S. Department of the Interior U.S. Geological Survey*, p. 46, 2007.

[42] M. Paternoster, "Boron isotopes in the Mount Vulture groundwaters southern Italy: constraints for the assessment of natural and anthropogenic contaminant sources," *Geofluids*, vol. 2019, Article ID 9107636, 2019.

[43] R. N. Clayton, I. Friedman, D. L. Graf, T. K. Mayeda, W. F. Meents, and N. F. Shimp, "The origin of saline formation waters: 1. Isotopic composition," *Journal of Geophysical Research*, vol. 71, no. 16, pp. 3869–3882, 1966.

[44] I. Clarke and P. Fritz, *Environmental Isotopes in Hydrogeology*, Lewis Publishers, New York, 1997.

[45] M. Paternoster, M. Liotta, and R. Favara, "Stable isotope ratios in meteoric recharge and groundwater at Mt. Vulture volcano, southern Italy," *Journal of Hydrology*, vol. 348, no. 1-2, pp. 87–97, 2008.

[46] G. Vespasiano, C. Apollaro, R. De Rosa et al., "The Small Spring Method (SSM) for the definition of stable isotope-elevation relationships in Northern Calabria (Southern Italy)," *Applied Geochemistry*, vol. 63, pp. 333–346, 2015.

[47] A. Longinelli and E. Selmo, "Isotopic composition of precipitation in Italy: a first overall map," *Journal of Hydrology*, vol. 270, no. 1-2, pp. 75–88, 2003.

[48] F. Schemmel, T. Mikes, B. Rojay, and A. Mulch, "The impact of topography on isotopes in precipitation across the Central Anatolian Plateau Turkey," *American Journal of Science*, vol. 313, no. 2, pp. 61–80, 2013.

[49] G. Mongelli, A. Argyraki, M. L. García Lorenzo, M. Wasif Shammout, M. Paternoster, and V. Simeone, "Groundwater quality in the Mediterranean region," *Geofluids*, vol. 2019, Article ID 7269304, 19 pages, 2019.

[50] P. Ravikumar, K. Venkatesharaju, and R. K. Somashekar, "Major ion chemistry and hydrochemical studies of groundwater of Bangalore South Taluk, India," *Environmental Monitoring and Assessment*, vol. 163, no. 1-4, pp. 643–653, 2010.

[51] M. Salifu, F. Aidoo, M. Saah Hayford, D. Adomako, and E. Asare, "Evaluating the suitability of groundwater for irrigational purposes in some selected districts of the Upper West region of Ghana," *Applied Water Science*, vol. 7, no. 2, pp. 653–662, 2017.

[52] K. S. Rawat, S. K. Singh, and S. K. Gautam, "Assessment of groundwater quality for irrigation use: a peninsular case study," *Applied Water Science*, vol. 8, no. 8, 2018.

[53] L. V. Wilcox, *Classification and Use of Irrigation Waters*, USDA. Circ 969, Washington, DC, USA, 1955.

[54] T. Subramani, L. Elango, and S. R. Damodarasamy, "Groundwater quality and its suitability for drinking and agricultural use in Chithar River Basin, Tamil Nadu, India," *Environmental Geology*, vol. 47, no. 8, pp. 1099–1110, 2005.

[55] A. Shahabi, M. J. Malakouti, and E. Fallahi, "Effects of bicarbonate content of irrigation water on nutritional disorders of some apple varieties," *Journal of Plant Nutrition*, vol. 28, no. 9, pp. 1663–1687, 2005.

[56] S. K. Gautam, C. Maharana, D. Sharma, A. K. Singh, J. K. Tripathi, and S. K. Singh, "Evaluation of groundwater quality in the Chotanagpur plateau region of the Subarnarekha River basin, Jharkhand State, India," *Sustainability of Water Quality and Ecology*, vol. 6, pp. 57–74, 2015.

[57] M. Al-Shammiri, A. Al-Saffar, S. Bohamad, and M. Ahmed, "Waste water quality and reuse in irrigation in Kuwait using microfiltration technology in treatment," *Desalination*, vol. 185, no. 1–3, pp. 213–225, 2005.

[58] R. Italiana, "Decreto Legislativo 2 febbraio 2001, n. 31 Attuazione della direttiva 98/83/CE relativa alla qualità delle acque destinate al consumo umano," *Gazzetta Ufficiale della Repubblica Italiana*, vol. 52, 2001.

[59] EU Directive, 1998/83/EC, "Council Directive of 3 November 1998 on the quality of water intended for human consumption," *Official Journal of the European Union L 330*, pp. 32–54, 1998.

[60] World Health Organization, *Guidelines for Drinking Water Quality: Training Pack*, WHO, Geneva, 2004.

[61] G. Malina, "Ecotoxicological and environmental problems associated with the former chemical plant in Tarnowskie Gory, Poland," *Toxicology*, vol. 205, no. 3, pp. 157–172, 2004.

[62] P. Negrel and H. Pauwels, "Interaction between different groundwaters in Brittany catchments (France): characterizing multiple sources through strontium- and sulphur isotope tracing," *Water, Air, & Soil Pollution*, vol. 151, no. 1–4, pp. 261–285, 2004.